Acta Pharmaceutica Sinica B 2015;5(6):544–553

HOSTED BY

Chinese Pharmaceutical Association
Institute of Materia Medica, Chinese Academy of Medical Sciences

Acta Pharmaceutica Sinica B

www.elsevier.com/locate/apsb
www.sciencedirect.com

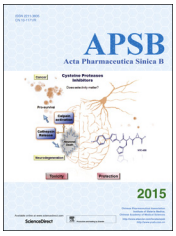

ORIGINAL ARTICLE

Fucoidan protects hepatocytes from apoptosis and inhibits invasion of hepatocellular carcinoma by up-regulating p42/44 MAPK-dependent NDRG-1/CAP43

Yuri Cho, Jung-Hwan Yoon*, Jeong-ju Yoo, Minjong Lee, Dong Hyeon Lee, Eun Ju Cho, Jeong-Hoon Lee, Su Jong Yu, Yoon Jun Kim, Chung Yong Kim

Department of Internal Medicine and Liver Research Institute, Seoul National University College of Medicine, Seoul, Korea

Received 26 June 2015; received in revised form 21 August 2015; accepted 7 September 2015

KEY WORDS

Fucoidan;
Hepatocellular carcinoma;
Invasion;
Hypoxia;
Hepatoprotective;
Cultured hepatocyte;
NDRG-1/CAP43;
VMP-1

Abstract Fucoidan is a traditional Chinese medicine suggested to possess anti-tumor effects. In this study the anti-metastatic effects of fucoidan were investigated *in vitro* in human hepatocellular carcinoma (HCC) cells (Huh-7 and SNU-761) under normoxic and hypoxic conditions and *in vivo* using a distant liver metastasis model involving injection of MH134 cells into spleen *via* the portal vein. Its ability to protect hepatocytes against bile acid (BA)-induced apoptosis was investigated in primary hepatocytes. Fucoidan was found to suppress the invasion of HCC cells through up-regulation of p42/44 MAPK-dependent NDRG-1/CAP43 and partly, under normoxic conditions, through up-regulation of p42/44 MAPK-dependent VMP-1 expression. It also significantly decreased liver metastasis *in vivo*. As regards its hepatoprotective effect, fucoidan decreased BA-induced hepatocyte apoptosis as shown by the attenuation of caspase-8, and -7 cleavages and suppression of the mobilization of caspase-8 and Fas associated death domain (FADD) into the death-inducing signaling complex. In summary, fucoidan

Abbreviations: BA, bile acid; cDNA, complementary DNA; CXCL, chemokine ligand; DISC, death-inducing signaling complex; DMEM, Dulbecco's modified Eagle's medium; DNA, deoxyribonucleic acid; ELISA, enzyme-linked immunosorbent assay; FADD, Fas associated death domain; FBS, fetal bovine serum; FCS, fetal calf serum; GAPDH, glyceraldehyde-3-phosphate dehydrogenase; GP, glypican; HCC, hepatocellular carcinoma; IHC, immunohistochemistry; JNK, c-Jun NH_2-terminal kinase; MAPK, mitogen-activated protein kinase; MTS, 3,4-(5-dimethylthiazol-2-yl)-5-(3-carboxymethoxyphenyl)-2-(4-sulfophenyl)-2*H*-tetrazolium salt; *NDRG*, N-myc downstream-regulated gene; PCR, polymerase chain reaction; RNA, ribonucleic acid; SD, standard deviation; SDS-PAGE, sodium dodecyl sulfate-polyacrylamide gel electrophoresis; siRNA, small interfering RNA; VMP, vacuole membrane protein; WME, William's medium E

*Corresponding author. Tel.: +82 2 2072 2228; fax: +82 2 743 6701.
E-mail address: yoonjh@snu.ac.kr (Jung-Hwan Yoon).

Peer review under responsibility of Institute of Materia Medica, Chinese Academy of Medical Sciences and Chinese Pharmaceutical Association.

http://dx.doi.org/10.1016/j.apsb.2015.09.004

displays inhibitory effects on proliferation of HCC cells and protective effects on hepatocytes. The results suggest fucoidan is a potent suppressor of tumor invasion with hepatoprotective effects.

1. Introduction

Hepatocellular carcinoma (HCC) is one of the most prevalent cancers worldwide[1]. It is difficult to treat because of its insensitivity to chemotherapy and rapid development of drug resistance[2]. Moreover, as HCC progresses, hydrophobic bile acids (BAs) accumulate during intrahepatic cholestasis and induce apoptosis of hepatocytes which ultimately results in liver cirrhosis or hepatic failure[3]. In fact the poor prognosis of HCC patients[4] is not due to the tumor itself but to the secondary hepatic decompensation[5] reflected in several functional HCC staging systems such as the Barcelona Clinic Liver Cancer System[6] and the Hong Kong Liver Cancer Staging System[7]. For this reason, the development of a potent HCC suppressor with a hepatoprotective effect would represent a marked improvement in the treatment of HCC.

Fucoidan is a family of sulphated polyfucose polysaccharides isolated from brown algae that exhibit anti-tumor[8–10], anti-thrombotic[11], anti-inflammatory[12] and anti-viral activities[13]. In particular, the anti-cancer effects and low toxicity of fucoidan make it a potentially valuable candidate for cancer chemotherapy[14]. Fucoidan effectively suppresses cancer cell proliferation *in vitro*[15], and inhibits metastasis and angiogenesis of B16 melanoma xenografts and Lewis lung adenocarcinomas *in vivo*[9,16]. More recently, it was reported to inhibit the growth of hepatoma Huh-7 cells through down-regulation of the chemokine ligand (CXCL)-12 at 1.0 mg/mL[17]. Nevertheless, the anti-metastatic effects of fucoidan remain to be fully evaluated.

Fucoidan has also been reported to exert a protective effect on hepatocytes showing anti-oxidative effects against acute liver injury and liver fibrosis[18,19]. Recently fucoidan was shown to protect against acetaminophen-associated liver injury *in vivo*[20]. However, the question of whether fucoidan has hepatoprotective effects against BA-induced apoptosis has not been investigated.

In the present study, the effects and mechanism of action of fucoidan in HCC cell invasion *in vitro* and *in vivo* and its hepatoprotective effect against BA were evaluated. In particular, given the importance of the hypoxic microenvironment to the survival of HCC cells[21,22], studies were carried out under normoxic and hypoxic conditions.

2. Materials and methods

2.1. Cell lines and cell culture conditions

Three human HCC cell lines were used in this study *viz* Huh-BAT (a well-differentiated BA-transporter transfected HCC cell line), Huh-7 (a well-differentiated HCC cell line), and SNU-761 (a poorly differentiated HCC cell line)[23–25]. Cells were grown in Dulbecco's modified Eagle's medium (DMEM) supplemented with 10% fetal bovine serum (FBS), 100,000 U/L penicillin, and 100 mg/L streptomycin with or without 100 nmol/L insulin. In all experiments, cells were subjected to overnight serum starvation to avoid confounding variables related to serum-induced signaling. Cells were incubated at 37 °C under either normoxic conditions (20% O_2, 5% CO_2) or hypoxic conditions (1% O_2, 5% CO_2 and 94% N_2). Fucoidan from *Fucus vesiculosus* was obtained from Sigma-Aldrich Co. LLC. (Seoul, South Korea).

2.2. Animal experiments

In vivo studies were carried out in C3H mice (Orient Bio Inc). The *in vivo* study protocol was approved by the Institutional Animal Care and Use Committee (IACUC) and Ethics Committee of Seoul National University Hospital, Central South University and all experiments were carried out in strict accordance with the recommendations of the Guide for the Care and Use of Laboratory Animals of the National Institutes of Health. Surgical procedures were performed under anesthesia with sodium pentobarbital unless otherwise stated and all efforts were made to minimize animal stress and suffering.

2.3. Cell proliferation analysis (MTS assay)

Cell proliferation was determined using the Cell Titer 96 Aqueous One Solution cell proliferation assay (Promega, Madison, WI, USA). This measures the conversion of the colorimetric reagent 3,4-(5-dimethylthiazol-2-yl)-5-(3-carboxymethoxyphenyl)-2-(4-sulfophenyl)-2*H*-tetrazolium salt (MTS) into soluble formazan by dehydrogenase enzymes found in metabolically proliferating cell. Following each treatment, 20 μL dye solution was added to each well of a 96-well plate and incubated for 2 h. Subsequently, absorbance was recorded at 490 nm using an enzyme-linked immunosorbent assay (ELISA) plate reader (Molecular Devices, Sunnyvale, CA, USA). The half maximal inhibitory concentration (IC_{50}) for each cell line was calculated using the Softmax Pro plate reader program.

2.4. Cell invasion assay

Invasion of HCC cells (Huh-7 and SNU-761) under both normoxic and hypoxic conditions was measured in 24-well chambers. Inserts were transferred into wells and coated with Matrigel (BD Biosciences, Billerica, MA, USA) for 30 min at 37 °C. Cells were then suspended in serum-free medium and implanted on the Matrigel-coated upper chambers (5×10^4 cells/chamber); DMEM containing 10% fetal bovine serum (FBS) was added to the lower chambers. Cells were incubated for 6 h at 37 °C and then incubated with or without fucoidan for 24 h before being stained with 4 μg/mL calcein AM (BD Biosciences, Billerica, MA, USA) in Hank's balanced salt solution (HBSS) at 37 °C for 90 min. Invasion capacity was determined as relative fluorescence units measured at excitation and emission wavelengths of 494 and 517 nm respectively using a multifunctional plate reader (EnVision Multilabel Reader; PerkinElmer Inc., Waltham, MA, USA).

2.5. Immunoblot analysis

HCC cells were lysed on ice for 20 min using lysis buffer and centrifuged at 14,000 × *g* for 10 min at 4 °C. To carry out sodium dodecyl sulfate polyacrylamide gel electrophoresis (SDS-PAGE), samples were transferred to nitrocellulose membranes, blotted with appropriate primary antibodies at a dilution of 1:1000, and treated with peroxidase-conjugated secondary antibodies (Biosource International, Camarillo, CA, USA). Bound antibodies were visualized using chemiluminescent substrate (ECL; Amersham, Arlington Heights, IL, USA) and exposed to Kodak X-OMAT film (Kodak, New Haven, CT, USA). Primary antibodies included: rabbit anti-phospho-p42/44 mitogen-activated protein kinase (MAPK), rabbit anti-caspase 9, 6, 3, and anti-caspase 7 (cleaved) (all from Cell Signaling Technology, Danvers, MA, USA); anti-caspase 8 (BD Biosciences, San Jose, CA, USA); rabbit anti-N-myc downstream-regulated gene (NDRG)-1/CAP43 (Invitrogen Corporation, Camarillo, CA, USA). Goat anti-actin antibody was from Santa Cruz Biotechnology Inc. (Santa Cruz, CA, USA). Densitometric analysis was performed with Image J software (National Institutes of Health, Bethesda, MD, USA).

2.6. Real-time polymerase chain reaction (PCR) analysis

Total ribonucleic acids (RNAs) were extracted from Huh-7 and SNU-761 cells using Trizol reagent (Invitrogen, Carlsbad, CA, USA). Complementary deoxyribonucleic acid (cDNA) templates were prepared using oligo(dT) random primers and Moloney murine leukemia virus (MoMLV) reverse transcriptase. After the reverse transcription reaction, the cDNA template was amplified by PCR using Taq polymerase (Invitrogen). *VMP-1* was determined by real-time PCR (LightCycler; Roche Molecular Biochemicals, Mannheim, Germany) using SYBR green as the fluorophore (Molecular Probes, Eugene, OR, USA). After electrophoresis in 1% agarose gel, the portion of gel containing the expected PCR product of vacuole membrane protein 1 (*VMP-1*) was excised (242 bp) and the product eluted into Tris–HCl buffer using a DNA gel extraction kit (Qiagen, Valencia, CA, USA). Forward and reverse primers were 5′-GTGGCTTTCATTGGTGCTGTCC-3′ and 5′-GAGTTCAACCGCTGCTGGA TTC-3′, respectively. Glyceraldehyde-3-phosphate dehydrogenase (*GAPDH*) gene expression was used as a control. The level of *VMP-1* mRNA expression was calculated as the relative intensity of the PCR product bands compared with that from the *GAPDH* gene using the $2^{-\Delta\Delta Ct}$ method. All PCR experiments were performed in triplicate.

2.7. SiRNA transfection

Cells were seeded in a 6-well culture plate (2×10^5 cells/well) in 2-mL antibiotic-free medium supplemented with 10% FBS. At 60%–80% confluence, cells were transfected with small interfering RNA (siRNA) using the siRNA transfection reagent (Santa Cruz Biotechnology Inc., Santa Cruz, CA, USA) according to the manufacturer's instructions. The cells were treated with siRNA for 6 h at 37 °C and then growth medium containing 20% FBS and antibiotics was added. After 18 h, the medium was replaced with fresh medium containing 10% FBS and antibiotics and after 24 h, the cells were used in subsequent experiments.

2.8. Distant metastasis model (splenic injection)

Five-week-old male C3H mice were anesthetized with ether and subjected to splenic injection as previously described[26]. After exposing the spleen by an upper quadrant incision, 1×10^5 MH134 cells (a mouse hepatocellular carcinoma cell line)[27] were injected into its lower pole using a 31-gauge needle. Mice were then treated with intraperitoneal (i.p.) injections of normal saline (control group, $n=4$) or 10 mg/kg fucoidan (treatment group, $n=4$) every two days. After eight days, the number of macroscopic liver metastases and the sum of the maximal diameter for each nodule were determined. The i.p. dose was determined based on a previous study of the antitumor effects of fucoidan *in vivo*[28]. Tumor specimens were fixed in 4% formaldehyde and embedded in paraffin. For immunohistochemical (IHC) analysis, specimens were cut into 4 μm sections and subjected to IHC staining using the anti-mouse CD31 antibody (Vector Laboratories, Inc., Burlingame, USA) at a 1:300 dilution or anti-glypican (GP)-3 antibody (Novus Biologicals, Littleton, USA) at a 1:200 dilution.

2.9. Primary hepatocyte isolation and culture

Primary hepatocytes from five-week-old C3H mice were isolated and cultured as previously described[29]. The mice were housed and handled under specific pathogen-free conditions. Hanks' solution I consisted of basal Hanks' solution containing 2.5 mmol/L EGTA, 0.1% glucose and penicillin/streptomycin at a dilution of 1:100. Hanks' solution II consisted of basal Hanks' solution containing 0.3 mg/mL collagenase CLSII and 5 mmol/L $CaCl_2$. Hanks' solutions were prewarmed to 42 °C and collagenase added immediately prior to liver perfusion. After shaving the abdomen, the abdominal cavity was opened and the portal vein cannulated with a 25-gauge catheter to which a silicon tube was connected. Hanks' solution I was perfused using a peristaltic infusion pump at a flow rate of 8 mL/min. After infusion was initiated, the inferior vena cava was incised to permit sufficient outflow. The liver was perfused with Hanks' solution I for 2 min followed by Hanks′ solution II for 5 min. Efficient perfusion *via* the portal vein was evidenced by the color change in liver from dark red-brown to light brown. Following perfusion, the gallbladder and liver capsule were removed using a pincette and livers transferred to sterile Petri dishes.

After disintegrating livers by gentle shaking, suspensions were filtered through a 100 mm cell strainer and transferred to 50 mL Falcon tubes. Cells were washed twice with William's medium E (WME) at room temperature and 37.5 °C before being centrifuged for 2 min and resuspended in WME. Hepatocytes were then plated on collagen-coated culture dishes with fetal calf serum (FCS) cell culture medium and kept in a humidified cell culture incubator at 37 °C under 5% CO_2. After 4 h during which hepatocytes attached to the collagen-coated dish, FCS medium was removed and replaced with serum-free cell culture medium. After a further 14–20 h, cells were washed three times with starvation medium and incubated in starvation medium for the indicated time periods.

2.10. Death-inducing signaling complex immunoprecipitation (DISC IP)

Cell pellets were treated with lysis buffer (100 mmol/L Tris–HCl, 5 μmol/L EDTA, and 1% NP-40) containing protease inhibitor

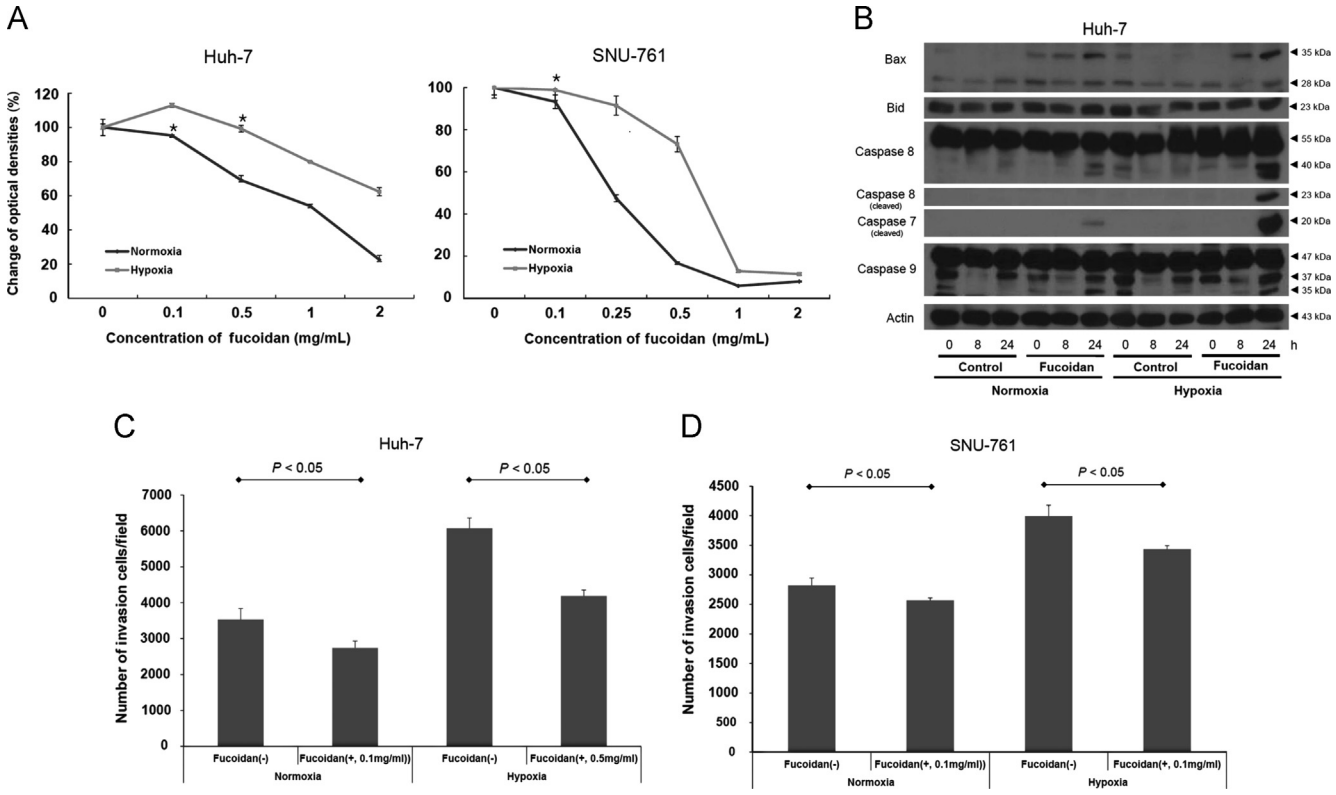

Figure 1 Effect of fucoidan on proliferation and invasion of HCC cells. (A) Huh-7 and SNU-761 cell growth following treatment with fucoidan (0, 0.1, 0.25, 0.5, 1, and 2 mg/mL). *Concentration used in the invasion assay; (B) Fucoidan (1 mg/mL) enhances apoptosis of Huh-7 cells under both normoxic and hypoxic conditions; (C) Huh-7 cell invasion through a Matrigel-coated filter following treatment with fucoidan 0.1 mg/mL under normoxic conditions and 0.5 mg/mL under hypoxic conditions; (D) SNU-761 cell invasion following treatment with fucoidan 0.1 mg/mL under both normoxic and hypoxic conditions.

and phosphatase inhibitor cocktails. Total protein (500 μg) was incubated with rat anti-death receptor (DR) 5 antibody (Santa Cruz Biotechnology Inc., Santa Cruz, CA, USA), mouse anti-Fas-associated death domain (FADD) antibody (BD Biosciences, San Jose, CA, USA), mouse anti-cellular FLICE inhibitory protein (cFLIP) antibody (Enzo Life Science, Farmingdale, NY, USA), or mouse anti-caspase 8 antibody (Upstate, Lake Placid, NY, USA) at 4 °C for 1 h. Protein A/G beads (Santa Cruz, San Diego, CA, USA) were added to the lysate and incubated overnight with gentle rocking at 4 °C. The beads were washed five times by repeated suspension in 500 μL lysis buffer followed by centrifugation at 10,000 × *g* for 1 min. After the last wash, 35 μL Laemmli buffer (4% SDS, 20% glycerol, 10% 2-mercaptoethanol, 0.004% bromophenol blue, 0.125 mol/L Tris HCl, pH 6.8) was added to the pellet and heated at 100 °C for 5 min. Centrifugation was performed again to collect supernatant and finally samples were subjected to immunoblot analysis as described above.

2.11. *Statistical analysis*

Statistical analysis was performed using PASW version 18.0 (SPSS Inc., Chicago, IL, USA). All experimental results are based on three independent experiments using cells from three separate isolations and are presented as mean ± standard deviation (SD). For comparisons between groups, data were analyzed by the Mann–Whitney U test or one-way ANOVA. For all tests, $P < 0.05$ was regarded as statistically significant.

3. Results

3.1. *Cell proliferation analysis (MTS assay)*

The effect of 0–2 mg/mL fucoidan on Huh-7 and SNU-761 cell growth was assessed *in vitro* using the MTS assay. Cell proliferation following fucoidan treatment decreased in a dose-dependent manner under both normoxic and hypoxic conditions (Fig. 1A). Moreover, 1 mg/mL fucoidan enhanced apoptosis of Huh-7 cells as compared to control as shown by the expression of bax, bid, caspase-8, -7, and -9 cleavages, under both normoxic and hypoxic conditions (Fig. 1B). The IC_{50} values in Huh-7 cells were estimated to be 0.80 mg/mL under normoxic conditions and 1.05 mg/mL under hypoxic conditions. Corresponding values in SNU-761 cells were 0.28 and 0.6 mg/mL, respectively.

3.2. *Cell invasion assay*

Invasion assays were performed using a concentration of fucoidan that did not inhibit proliferation of HCC cells (Huh-7 and SNU-761) under normoxic and hypoxic conditions. Huh-7 cell invasion through a Matrigel-coated filter was evaluated after treatment with fucoidan 0.1 mg/mL under normoxic conditions and 0.5 mg/mL under hypoxic conditions. SNU-761 cell invasion was evaluated after treatment with fucoidan 0.1 mg/mL under both normoxic and hypoxic conditions. At 24 h, fucoidan significantly suppressed Huh-7 and SNU-761 cell invasion compared to controls under both normoxic and hypoxic conditions (Fig. 1C and D).

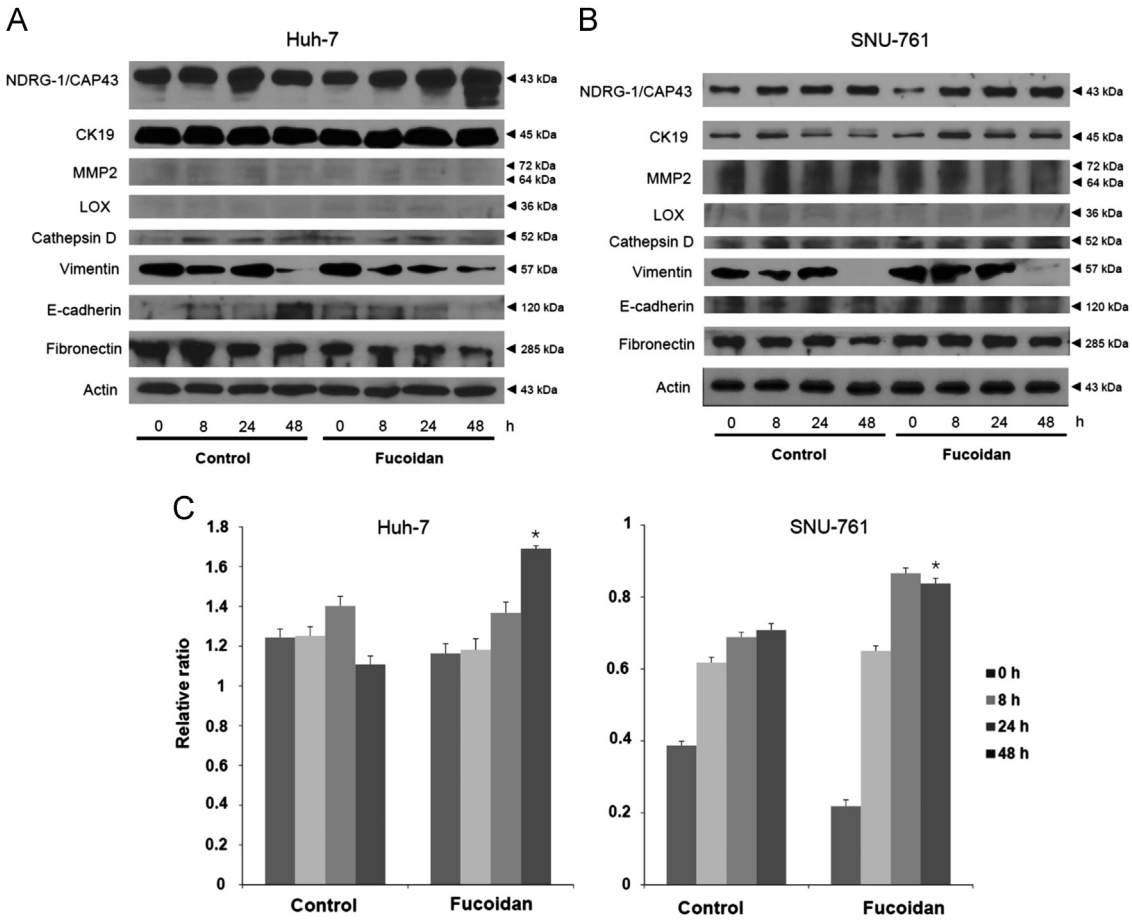

Figure 2 Fucoidan enhances the expression of NDRG-1/CAP43 and mesenchymal markers. Expression of NDRG-1/CAP43 and mesenchymal markers (CK19, MMP-2, LOX, cathepsin D, vimentin, e-cadherin and fibronectin) were evaluated by immunoblotting in (A) Huh-7 and (B) SNU-761 cells and by (C) densitometric analyses (data are expressed as the relative ratio of NDRG-1/CAP43 to actin).

3.3. Enhanced p42/44 MAPK pathway dependent NDRG/CAP43 by fucoidan

The expressions of NDRG-1/CAP43 (a stress-responsive protein involved in cell growth that acts as a tumor suppressor in many cell types) and mesenchymal markers (CK19, MMP-2, MMP-9, LOX, cathepsin D, vimentin, E-cadherin, and fibronectin) were evaluated by immunoblotting. The expression of NDRG-1/CAP43 was higher in Huh-7 and SNU-761 cells treated with fucoidan than in controls at 48 h (Fig. 2A and B). The up-regulation of NDRG-1/CAP43 expression in fucoidan-treated SNU-761 cells was slightly less prominent which may be due to the different cell lines. Increased expression of NDRG-1/CAP43 at 48 h due to fucoidan was also found by densitometric analysis (Fig. 2C). In contrast, fucoidan treatment was found to decrease the expressions of vimentin, E-cadherin, and fibronectin in Huh-7 cells as compared to controls (Fig. 2A).

In order to determine the pathway activated by fucoidan, the expressions of total p42/44, phosphorylated-p42/44 (p-p42/44), total Akt, and phosphorylated-Akt (p-Akt) were evaluated in HCC cells by immunoblot assay. At early time points, the expression of p-p42/44 was higher in Huh-7 cells compared to control cells (Fig. 3A) and expression was also higher in SNU-761 cells (Fig. 3B). However, changes in the expression of total Akt and p-Akt were not consistent in the two cell lines.

The effect of fucoidan on the expression of p42/44 MAPK pathway-dependent NDRG-1/CAP43 in Huh-7 and SNU-761 cells was also evaluated by immunoblotting and found to be attenuated by U0126 (MAPK inhibitor) treatment (Fig. 3C). Densitometric analysis also confirmed that fucoidan activates the expression of NDRG-1/CAP43 in a p42/44 MAPK pathway-dependent manner (Fig. 3D).

An invasion assay was also carried out to evaluate whether NDRG-1/CAP43 siRNA increases invasion of fucoidan-treated HCC cells. First, the specific knockdown effect of siRNA targeting NDRG-1/CAP43 was examined by immunoblot assay. As shown in Fig. 4A, NDRG-1/CAP43 siRNA significantly decreased the expression of NDRG-1/CAP43 in Huh-7 cells. In addition, fucoidan suppressed HCC cell invasion *via* NDRG-1/CAP43 under both normoxic and hypoxic conditions (Fig. 4B and C).

3.4. Enhanced expression of VMP-1 by fucoidan under normoxic conditions

The effect of fucoidan treatment on *VMP-1* (a novel molecule that inhibits metastasis and proliferation in HCC) was investigated using quantitative real-time PCR. *VMP-1* mRNA expression was significantly increased in SNU-761 cells (Fig. 5A), *VMP-1* siRNA significantly decreased *VMP-1* mRNA expression in both Huh-7

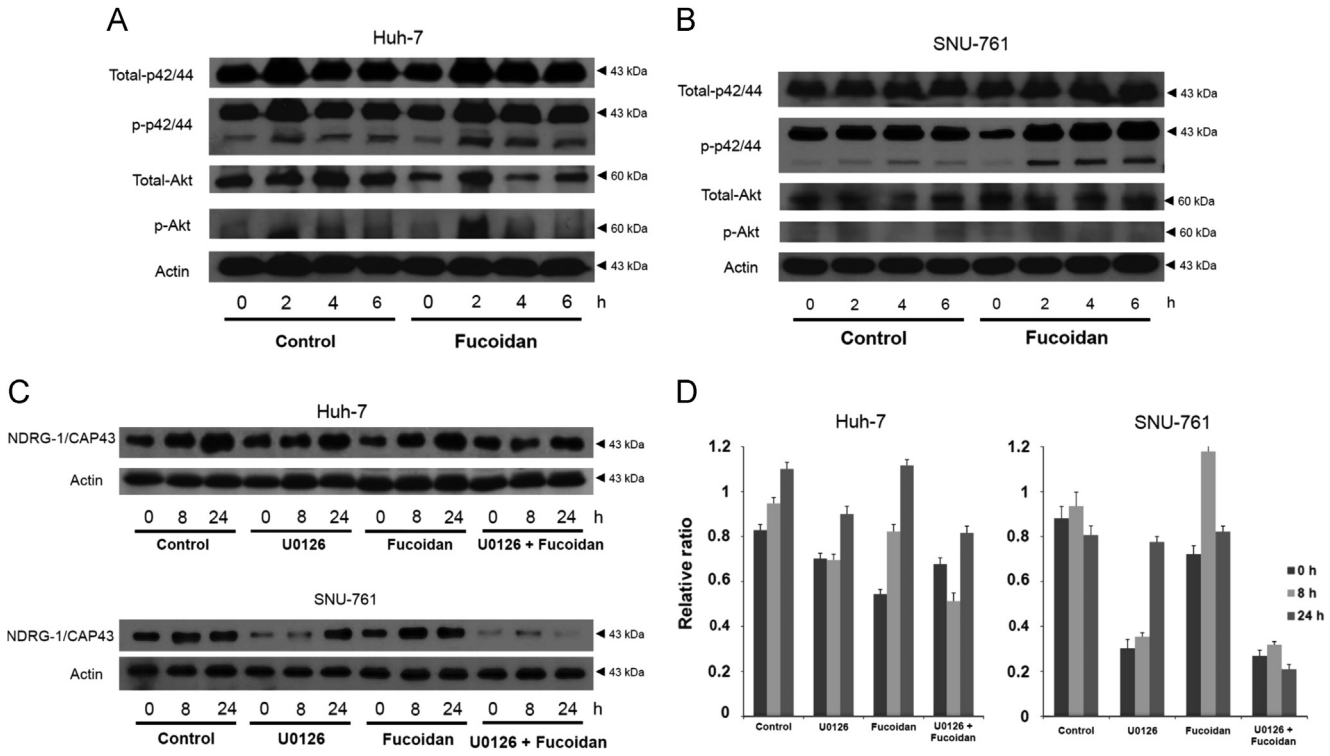

Figure 3 Fucoidan enhances the expression of NDRG-1/CAP43 by the p42/44 MAPK pathway. Immunoblotting reveals that fucoidan enhances expression of phosphorylated-p42/44 (p-p42/44) in (A) Huh-7 and (B) SNU-761 cells and (C) that expression of NDRG-1/CAP43 in Huh-7 and SNU-761 cells is attenuated by treatment with U0126 (MAPK inhibitor). (D) The outcome of densitometric analysis data are expressed as the relative ratio of NDRG-1/CAP43 to actin.

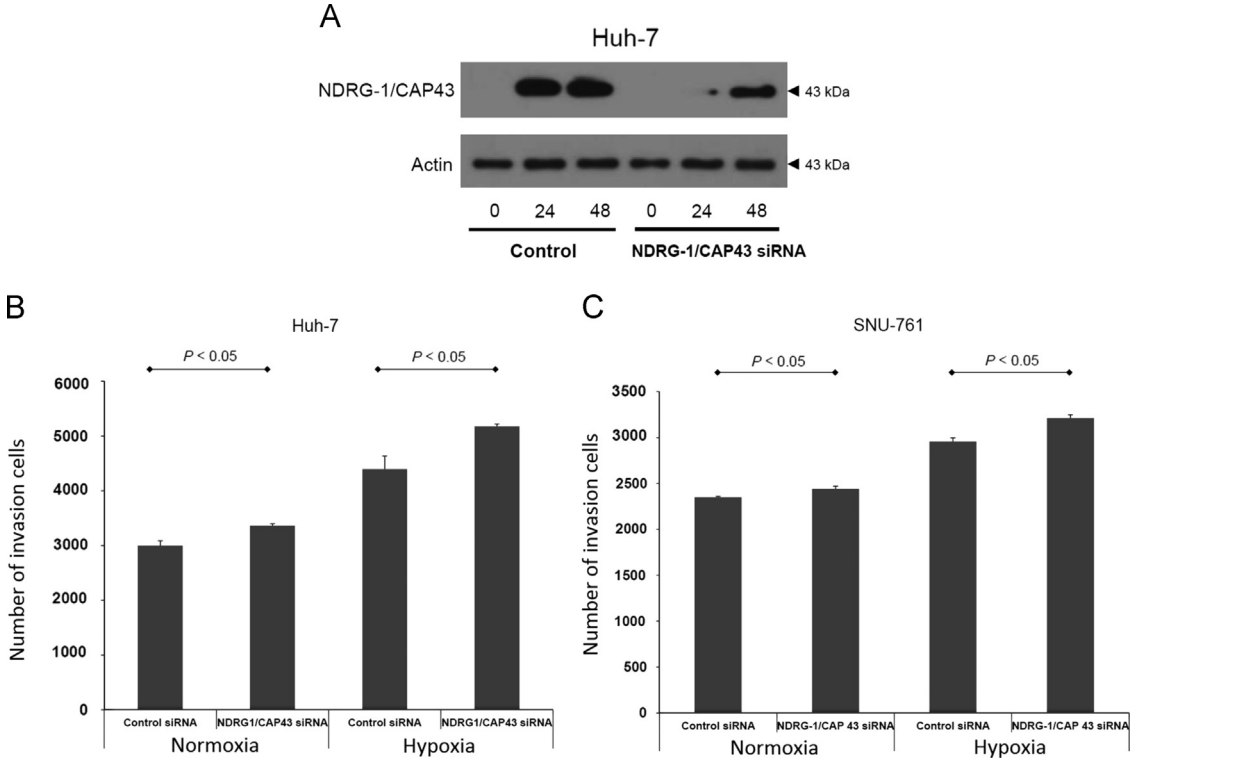

Figure 4 Invasion of HCC cells following fucoidan treatment with NDRG-1/CAP43 siRNA. (A) Immunoblot analysis reveals that NDRG-1/CAP43 siRNA significantly decreases the expression of NDRG-1/CAP43 in Huh-7 cells and increased invasion of fucoidan-treated HCC cells. Fucoidan suppresses invasion of (B) Huh-7 and (C) SNU-761 cells through NDRG-1/CAP43 activity.

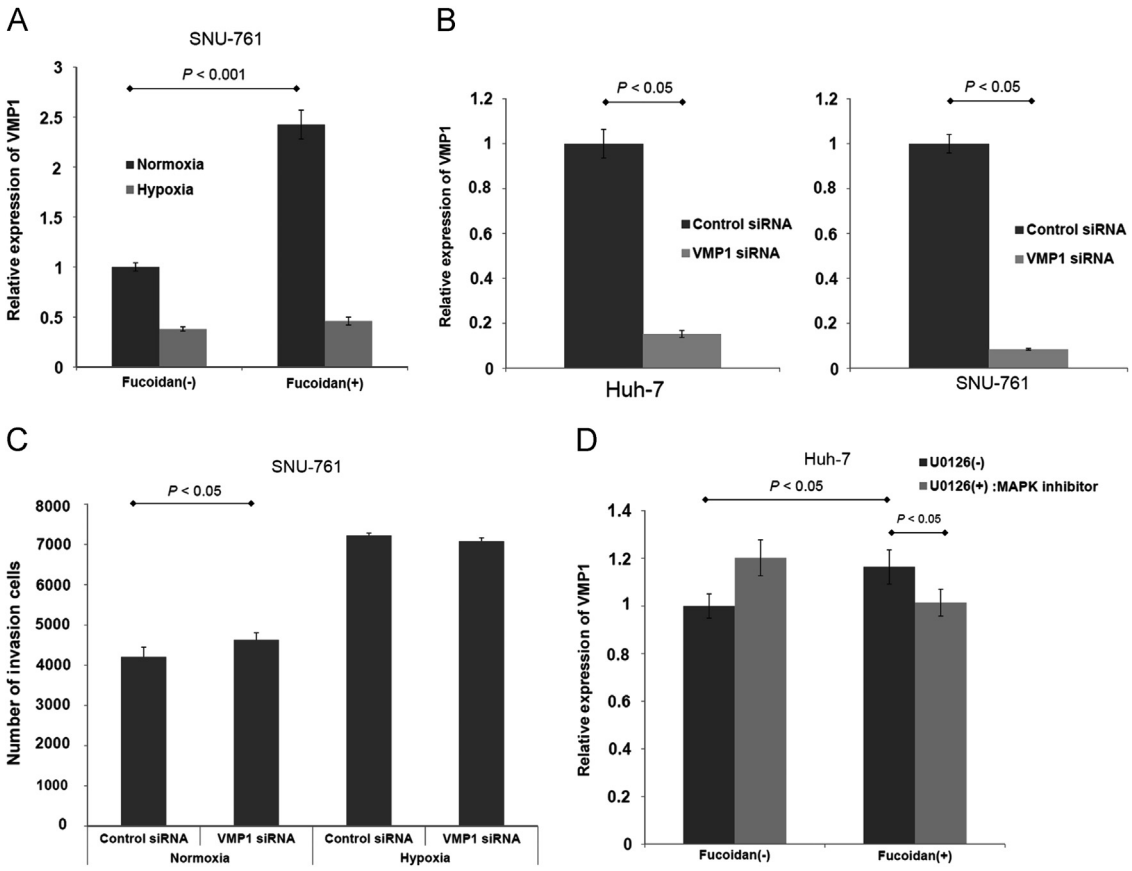

Figure 5 Fucoidan enhances expression of VMP-1 under normoxic conditions. (A) RT-PCR reveals that fucoidan significantly increases VMP-1 mRNA expression; (B) VMP-1 siRNA significantly decreases VMP-1 mRNA expression in both Huh-7 and SNU-761 cells; (C) VMP-1 siRNA increases invasion of fucoidan-treated HCC cells; (D) increased expression of VMP-1 in Huh-7 cells is attenuated by U0126 (MAPK inhibitor).

and SNU-761 cells (Fig. 5B, $P<0.05$) and *VMP-1* siRNA increased invasion of SNU-761 cells (Fig. 5C), all under normoxic conditions. Thus VMP-1 appears to be involved in HCC cell invasion but only under normoxic conditions. The increased expression of VMP-1 in Huh-7 cells was attenuated by U0126 (MAPK inhibitor) under normoxic conditions (Fig. 5D, $P<0.05$).

3.5. *Fucoidan inhibited liver metastasis in an intrahepatic portal vein metastasis model in vivo*

Fucoidan was anti-metastatic in the distant metastasis model as shown by the fact that the number of intrahepatic metastases in the fucoidan treatment group was significantly lower than in the control group (Fig. 6A, $P<0.05$). In addition, the sum of the maximal diameter of each nodule in the fucoidan treatment group was significantly lower than that in the control group (Fig. 6B, $P<0.05$). Fucoidan attenuated the nuclear grade of MH134 cells as determined by hematoxylin and eosin (H&E) staining and attenuated angiogenesis of MH134 cells as shown by decreased CD31 expression on IHC staining (Fig. 6C). The expression of GP-3 was also attenuated by fucoidan treatment when compared to control.

3.6. *Fucoidan suppressed BA-induced apoptosis*

To evaluate whether fucoidan decreased BA-induced hepatocyte apoptosis, the hepatoprotective effect of fucoidan on Huh-BAT cells stably transfected with a BA transporter was evaluated as previously described[30–32]. Fucoidan significantly decreased BA-induced Huh-BAT cell apoptosis as shown by attenuation of caspase-8, -9, -3, and -7 cleavages, p-JNK, and bid as compared to BA-treated cells (Fig. 7A). DISC-IP was used to evaluate changes in DISC assembly and revealed that fucoidan suppressed the mobilization of caspase-8, cFLIP, DR-5 and FADD into DISC as compared to BA-treated cells (Fig. 7B). Decreased recruitment to DISC leads to suppression of autocatalytic processes of the procaspases within DISC. Finally, following BA treatment of primary mouse hepatocytes in culture, immunoblotting showed fucoidan significantly decreased BA-induced hepatocyte apoptosis as shown by the attenuation of caspase-8, and -7 cleavages compared to BA-treated cells (Fig. 7C).

4. Discussion

The present study clearly demonstrates that fucoidan, a sulphated polysaccharide purified from brown algae, possesses anti-metastatic effects on HCC both *in vitro* (Huh-7 and SNU-761 cells) and *in vivo* (C3H mouse) and exerts a hepatoprotective effect by decreasing BA-induced hepatocyte apoptosis. Fucoidan inhibited HCC cell invasion through up-regulation of p42/44 MAPK-dependent NDRG-1/CAP43 and partly, under normoxic conditions, through up-regulation of p42/44 MAPK-dependent VMP-1. Fucoidan also decreased the migratory potential of Huh-7 cells by suppressing mesenchymal markers. *In vivo*, fucoidan decreased the

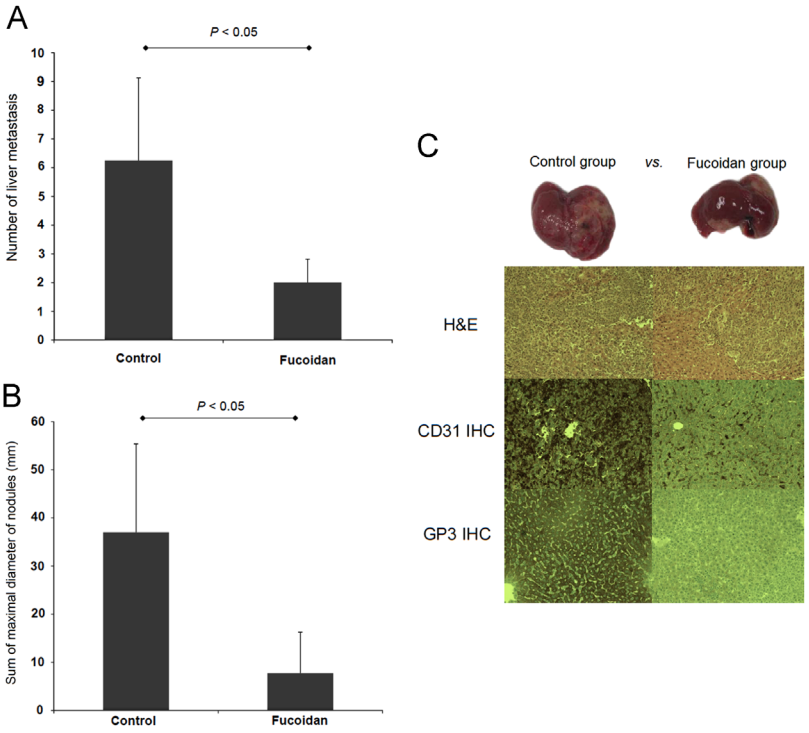

Figure 6 Fucoidan inhibits liver metastasis in the distant metastasis model. (A) The number of intrahepatic metastases in the fucoidan treatment group and control group; (B) the sum of the maximal diameter of each nodule in the two groups; (C) histological analysis following fucoidan treatment. The nuclear grade of MH134 cells was determined by H&E-staining and CD31 and GP-3 expression by IHC staining (200 ×).

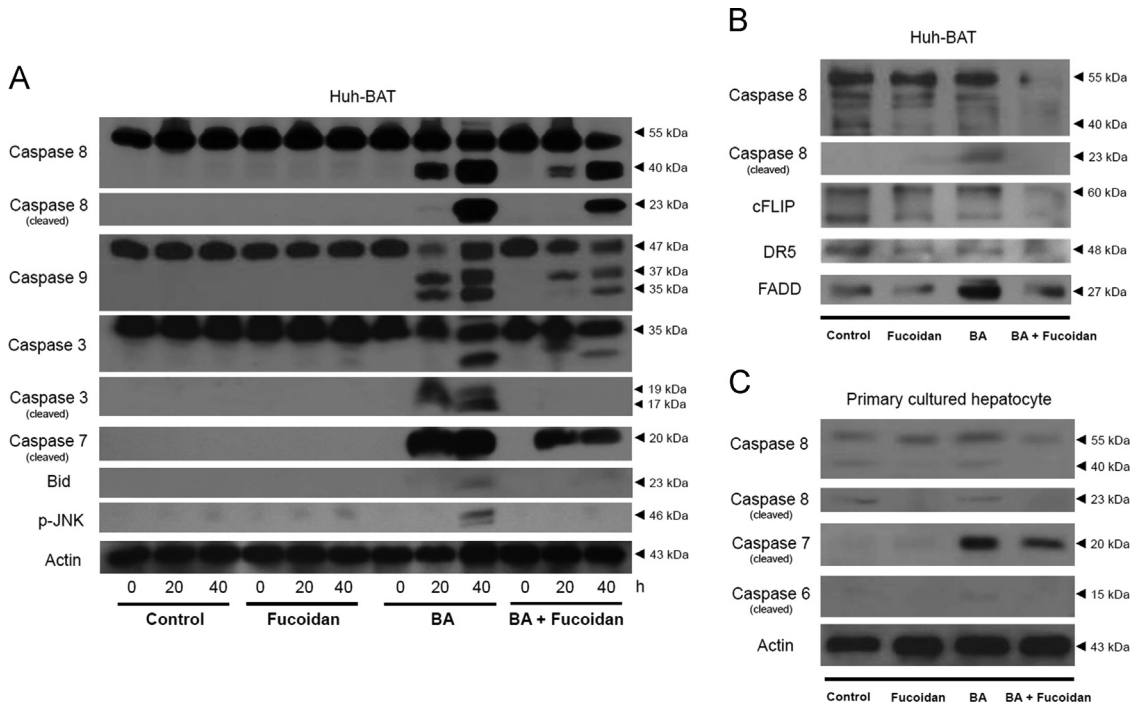

Figure 7 Fucoidan suppresses BA-induced hepatocyte apoptosis. (A) Suppression of BA-induced Huh-BAT cell apoptosis is shown by the attenuation of caspase-8, -9, -3, and -7 cleavages, p-JNK, and bid as compared to control; (B) Suppression of the mobilization of caspase-8, cFLIP, and FADD into DISC is shown by DISC-IP; (C) the decrease in BA-induced primary cultured-hepatocyte apoptosis as compared to BA-treated cells.

expression of the angiogenesis marker CD31. It also reduced the expression of GP-3 which correlates with poorly-differentiated HCC and poor prognosis[33,34].

NDRG-1/CAP43 (also known as Drg-1, RTP, Rit42 and PROXY-1) regulates tumor progression in various cancers and is involved in cell differentiation[35]. It is mainly expressed in non-

neoplastic tissue where it is regulated by hypoxia, oxidative stress, histone deacetylase-targeting drug, lysophosphatidylcholine, oncogene, and tumor suppressor gene[36,37]. Although some studies have reported conflicting results, NDRG-1/CAP43 appears to be a tumor suppressor or metastasis suppressor in many cancer cells including those of breast, prostate, cervical, ovarian and pancreatic cancers[38–42]. In this study, knockdown of NDRG-1/CAP43 significantly enhanced the invasion of HCC cells and its expression was modulated by the p42/44 MAPK pathway.

As previously reported, VMP-1 is an inhibitor of cell proliferation and secretory membrane transport. Moreover, it is necessary for autophagy and its expression induces the formation of autophagosomes[43]. Interestingly, VMP-1 was significantly up-regulated under normoxic conditions in this study. VMP-1 was recently identified as a membrane protein putatively associated with suppression of HCC growth and pulmonary metastases[44]. Based on our results, fucoidan appears to exert anti-metastatic effects by up-regulation of NDRG-1/CAP43 and VMP-1 in a p42/44 MAPK pathway-dependent manner.

The MAPK pathway usually controls proliferation of normal and tumor cells by activation of RAS, Raf and p42/44 but there have been some conflicting reports[45]. Very high signal intensity of p42/44 interrupts the cell cycle by inducing cell cycle inhibitors including $p21^{Cip/Waf}$ and $p27^{KIP}$[46]. This suggests that high signal intensity of p42/44 MAPK exerts a paradoxical effect on tumors. In the present study, fucoidan was shown to exert anti-metastatic effects on HCC cells by activating the p42/44 MAPK pathway.

Surprisingly, fucoidan decreased BA-induced apoptosis of hepatocytes while enhancing apoptosis of HCC cells. This dual ability to preserve hepatic function may represent an ideal strategy to treat HCC. The cytotoxic effects of hydrophobic BAs on normal hepatocytes have been well documented and previous studies have shown that mitochondrial dysfunction due to oxidative stress and the non-mitochondrial nitric oxide-dependent pathway result in hepatocyte apoptosis[47,48]. Procaspases are recruited to DISC *via* homotypic interactions between death effector domains (DED) of FADD and initiator caspases[49] and, once recruited, undergo autocatalytic processing[50]. Both the recruitment and processing is regulated by cFLIP[51]. A potential mechanism by which toxic BA promote death receptor cytotoxic signaling is by modulating the composition of DISC[52]. The results of our DISC IP studies suggest fucoidan suppresses these cascades.

5. Conclusions

We have demonstrated that fucoidan displays anti-metastatic effects on HCC through up-regulation of p42/44 MAPK-dependent NDRG-1/CAP43 and protects against BA-induced apoptosis of hepatocytes. This ability to suppress tumor invasion and exert hepatoprotective effects suggests fucoidan may represent an ideal therapeutic agent for the treatment of patients with HCC.

References

1. El-Serag HB, Mason AC. Rising incidence of hepatocellular carcinoma in the United States. *N Engl J Med* 1999;**340**:745–50.
2. Llovet JM, Ricci S, Mazzaferro V, Hilgard P, Gane E, Blanc JF, et al. Sorafenib in advanced hepatocellular carcinoma. *N Engl J Med* 2008;**359**:378–90.
3. Jang ES, Yoon JH, Lee SH, Lee SM, Lee JH, Yu SJ, et al. Sodium taurocholate cotransporting polypeptide mediates dual actions of deoxycholic acid in human hepatocellular carcinoma cells: enhanced apoptosis versus growth stimulation. *J Cancer Res Clin Oncol* 2014;**140**:133–44.
4. Guicciardi ME, Gores GJ. Bile acid-mediated hepatocyte apoptosis and cholestatic liver disease. *Dig Liver Dis* 2002;**34**:387–92.
5. Lee JH, Kim HY, Kim YJ, Yoon JH, Chung JW, Lee HS. BCLC system provides the best discrimination ability for survival of untreated hepatocellular carcinoma patients in an HBV-endemic area. *J Gastroenterol Hepatol* 2015;**30**:696–705.
6. European Association for Study of Liver, European Organisation for Research and Treatment of Cancer. EASL-EORTC clinical practice guidelines: management of hepatocellular carcinoma. *J Hepatol* 2012;**56**:908–43.
7. Yau T, Tang VY, Yao TJ, Fan ST, Lo CM, Poon RT. Development of Hong Kong Liver Cancer staging system with treatment stratification for patients with hepatocellular carcinoma. *Gastroenterology* 2014;**146** (e3):1691–700.
8. Parish CR, Coombe DR, Jakobsen KB, Bennett FA, Underwood PA. Evidence that sulphated polysaccharides inhibit tumour metastasis by blocking tumour-cell-derived heparanases. *Int J Cancer* 1987;**40**:511–8.
9. Koyanagi S, Tanigawa N, Nakagawa H, Soeda S, Shimeno H. Oversulfation of fucoidan enhances its anti-angiogenic and antitumor activities. *Biochem Pharmacol* 2003;**65**:173–9.
10. Maruyama H, Tamauchi H, Hashimoto M, Nakano T. Antitumor activity and immune response of Mekabu fucoidan extracted from sporophyll of *Undaria pinnatifida*. *In Vivo* 2003;**17**:245–9.
11. Trento F, Cattaneo F, Pescador R, Porta R, Ferro L. Antithrombin activity of an algal polysaccharide. *Thromb Res* 2001;**102**:457–65.
12. Tissot B, Daniel R. Biological properties of sulfated fucans: the potent inhibiting activity of algal fucoidan against the human compliment system. *Glycobiology* 2003;**13**:29G–30G.
13. McClure MO, Moore JP, Blanc DF, Scotting P, Cook GM, Keynes RJ, et al. Investigations into the mechanism by which sulfated polysaccharides inhibit HIV infection *in vitro*. *AIDS Res Hum Retroviruses* 1992;**8**:19–26.
14. Ikeguchi M, Yamamoto M, Arai Y, Maeta Y, Ashida K, Katano K, et al. Fucoidan reduces the toxicities of chemotherapy for patients with unresectable advanced or recurrent colorectal cancer. *Oncol Lett* 2011;**2**:319–22.
15. Ermakova S, Sokolova R, Kim SM, Um BH, Isakov V, Zvyagintseva T. Fucoidans from brown seaweeds *Sargassum hornery*, *Eclonia cava*, *Costaria costata*: structural characteristics and anticancer activity. *Appl Biochem Biotechnol* 2011;**164**:841–50.
16. Alekseyenko TV, Zhanayeva SY, Venediktova AA, Zvyagintseva TN, Kuznetsova TA, Besednova NN, et al. Antitumor and antimetastatic activity of fucoidan, a sulfated polysaccharide isolated from the Okhotsk Sea *Fucus evanescens* brown alga. *Bull Exp Biol Med* 2007;**143**:730–2.
17. Nagamine T, Hayakawa K, Kusakabe T, Takada H, Nakazato K, Hisanaga E, et al. Inhibitory effect of fucoidan on Huh7 hepatoma cells through downregulation of CXCL12. *Nutr Cancer* 2009;**61**:340–7.
18. Kang KS, Kim ID, Kwon RH, Lee JY, Kang JS, Ha BJ. The effects of fucoidan extracts on CCl_4-induced liver injury. *Arch Pharm Res* 2008;**31**:622–7.
19. Hong SW, Jung KH, Lee HS, Zheng HM, Choi MJ, Lee C, et al. Suppression by fucoidan of liver fibrogenesis *via* the TGF-beta/Smad pathway in protecting against oxidative stress. *Biosci Biotechnol Biochem* 2011;**75**:833–40.
20. Hong SW, Lee HS, Jung KH, Lee H, Hong SS. Protective effect of fucoidan against acetaminophen-induced liver injury. *Arch Pharm Res* 2012;**35**:1099–105.
21. Yoshiji H, Kuriyama S, Yoshii J, Ikenaka Y, Noguchi R, Hicklin DJ, et al. Synergistic effect of basic fibroblast growth factor and vascular endothelial growth factor in murine hepatocellular carcinoma. *Hepatology* 2002;**35**:834–42.

22. Gwak GY, Yoon JH, Kim KM, Lee HS, Chung JW, Gores GJ. Hypoxia stimulates proliferation of human hepatoma cells through the induction of hexokinase II expression. *J Hepatol* 2005;**42**:358–64.
23. Nakabayashi H, Taketa K, Miyano K, Yamane T, Sato J. Growth of human hepatoma cells lines with differentiated functions in chemically defined medium. *Cancer Res* 1982;**42**:3858–63.
24. Park JG, Lee JH, Kang MS, Park KJ, Jeon YM, Lee HJ, et al. Characterization of cell lines established from human hepatocellular carcinoma. *Int J Cancer* 1995;**62**:276–82.
25. Lee JH, Ku JL, Park YJ, Lee KU, Kim WH, Park JG. Establishment and characterization of four human hepatocellular carcinoma cell lines containing hepatitis B virus DNA. *World J Gastroenterol* 1999;**5**:289–95.
26. Arakawa Y, Shimada M, Utsunomiya T, Imura S, Morine Y, Ikemoto T. Effects of pegylated interferon α2b on metastasis of hepatocellular carcinoma. *J Surg Res* 2012;**172**:95–101.
27. Yamashita YI, Shimada M, Hasegawa H, Minagawa R, Rikimaru T, Hamatsu T, et al. Electroporation-mediated interleukin-12 gene therapy for hepatocellular carcinoma in the mice model. *Cancer Res* 2001;**61**:1005–12.
28. Xue M, Ge Y, Zhang J, Wang Q, Hou L, Liu Y, et al. Anticancer properties and mechanisms of fucoidan on mouse breast cancer *in vitro* and *in vivo*. *PLoS one* 2012;**7**:e43483.
29. Klingmuller U, Bauer A, Bohl S, Nickel PJ, Breitkopf K, Dooley S, et al. Primary mouse hepatocytes for systems biology approaches: a standardized *in vitro* system for modelling of signal transduction pathways. *Syst Biol* 2006;**153**:433–47.
30. Gwak GY, Moon TG, Lee DH, Yoo BC. Glycyrrhizin attenuates HMGB1-induced hepatocyte apoptosis by inhibiting the p38-dependent mitochondrial pathway. *World J Gastroenterol* 2012;**18**:679–84.
31. Yang JI, Yoon JH, Myung SJ, Gwak GY, Kim W, Chung GE, et al. Bile acid-induced TGR5-dependent c-Jun-N terminal kinase activation leads to enhanced caspase 8 activation in hepatocytes. *Biochem Biophys Res Commun* 2007;**361**:156–61.
32. Park SC, Yoon JH, Kim W, Gwak GY, Kim KM, Lee SH, et al. Eupatilin attenuates bile acid-induced hepatocyte apoptosis. *J Gastroenterol* 2006;**41**:772–8.
33. Shafizadeh N, Ferrell LD, Kakar S. Utility and limitations of glypican-3 expression for the diagnosis of hepatocellular carcinoma at both ends of the differentiation spectrum. *Mod Pathol* 2008;**21**:1011–8.
34. Shirakawa H, Suzuki H, Shimomura M, Kojima M, Gotohda N, Takahashi S, et al. Glypican-3 expression is correlated with poor prognosis in hepatocellular carcinoma. *Cancer Sci* 2009;**100**:1403–7.
35. Chen S, Han YH, Zheng Y, Zhao M, Yan H, Zhao Q, et al. NDRG1 contributes to retinoic acid-induced differentiation of leukemic cells. *Leuk Res* 2009;**33**:1108–13.
36. Zhou D, Salnikow K, Costa M. *Cap43*, a novel gene specifically induced by Ni^{2+} compounds. *Cancer Res* 1998;**58**:2182–9.
37. Shimono A, Okuda T, Kondoh H. N-myc-dependent repression of *Ndr1*, a gene identified by direct subtraction of whole mouse embryo cDNAs between wild type and *N-myc* mutant. *Mech Dev* 1999;**83**:39–52.
38. Bandyopadhyay S, Pai SK, Gross SC, Hirota S, Hosobe S, Miura K, et al. The *Drg-1* gene suppresses tumor metastasis in prostate cancer. *Cancer Res* 2003;**63**:1731–6.
39. Zhao G, Chen J, Deng Y, Gao F, Zhu J, Feng Z, et al. Identification of NDRG1-regulated genes associated with invasive potential in cervical and ovarian cancer cells. *Biochem Biophys Res Commun* 2011;**408**:154–9.
40. Angst E, Dawson DW, Stroka D, Gloor B, Park J, Candinas D, et al. N-myc downstream regulated gene-1 expression correlates with reduced pancreatic cancer growth and increased apoptosis *in vitro* and *in vivo*. *Surgery* 2011;**149**:614–24.
41. Akiba J, Murakami Y, Noda M, Watari K, Ogasawara S, Yoshida T, et al. N-myc downstream regulated gene 1/Cap43 overexpression suppresses tumor growth by hepatic cancer cells through cell cycle arrest at the G0/G1 phase. *Cancer Lett* 2011;**310**:25–34.
42. Kovacevic Z, Sivagurunathan S, Mangs H, Chikhani S, Zhang D, Richardson DR. The metastasis suppressor, N-myc downstream regulated gene 1 (*NDRG1*), upregulates p21 *via* p53-independent mechanisms. *Carcinogenesis* 2011;**32**:732–40.
43. Ropolo A, Grasso D, Pardo R, Sacchetti ML, Archange C, Lo Re A, et al. The pancreatitis-induced vacuole membrane protein 1 triggers autophagy in mammalian cells. *J Biol Chem* 2007;**282**:37124–33.
44. Guo L, Yang LY, Fan C, Chen GD, Wu F. Novel roles of Vmp1: inhibition metastasis and proliferation of hepatocellular carcinoma. *Cancer Sci* 2012;**103**:2110–9.
45. Boldt S, Weidle UH, Kolch W. The role of MAPK pathways in the action of chemotherapeutic drugs. *Carcinogenesis* 2002;**23**:1831–8.
46. Marshall C. How do small GTPase signal transduction pathways regulate cell cycle entry? *Curr Opin Cell Biol* 1999;**11**:732–6.
47. Yerushalmi B, Dahl R, Devereaux MW, Gumpricht E, Sokol RJ. Bile acid-induced rat hepatocyte apoptosis is inhibited by antioxidants and blockers of the mitochondrial permeability transition. *Hepatology* 2001;**33**:616–26.
48. Gumpricht E, Dahl R, Yerushalmi B, Devereaux MW, Sokol RJ. Nitric oxide ameliorates hydrophobic bile acid-induced apoptosis in isolated rat hepatocytes by non-mitochondrial pathways. *J Biol Chem* 2002;**277**:25823–30.
49. Bodmer JL, Holler N, Reynard S, Vinciguerra P, Schneider P, Juo P, et al. TRAIL receptor-2 signals apoptosis through FADD and caspase-8. *Nat Cell Biol* 2000;**2**:241–3.
50. Thornberry NA, Lazebnik Y. Caspases: enemies within. *Science* 1998;**281**:1312–6.
51. Rasper DM, Vaillancourt JP, Hadano S, Houtzager VM, Seiden I, Keen SL, et al. Cell death attenuation by 'Usurpin', a mammalian DED-caspase homologue that precludes caspase-8 recruitment and activation by the CD-95 (Fas, APO-1) receptor complex. *Cell Death Differ* 1998;**5**:271–88.
52. Higuchi H, Yoon JH, Grambihler A, Werneburg N, Bronk SF, Gores GJ. Bile acids stimulate cFLIP phosphorylation enhancing TRAIL-mediated apoptosis. *J Biol Chem* 2003;**278**:454–61.